IOPscience iopscience.iop.org

Miniaturized rotating disc rheometer test for rapid screening of drag reducing marine coatings

This content has been downloaded from IOPscience. Please scroll down to see the full text.

View the table of contents for this issue, or go to the journal homepage for more

Download details:

IP Address: 148.197.98.180
This content was downloaded on 11/05/2016 at 15:13

Please note that terms and conditions apply.

Surface Topography: Metrology and Properties

PAPER

Miniaturized rotating disc rheometer test for rapid screening of drag reducing marine coatings

Simon Dennington[1], **Ponkrit Mekkhunthod**[1], **Martin Rides**[2], **David Gibbs**[1,4], **Maria Salta**[1,5], **Victoria Stoodley**[3], **Julian Wharton**[1] **and Paul Stoodley**[1,6]

[1] National Centre for Advanced Tribology at Southampton (nCATS), Engineering Sciences, University of Southampton, Highfield, Southampton SO17 1BJ, UK
[2] National Physical Laboratory, Hampton Rd, Teddington, Middlesex TW11 0LW, UK
[3] Engineering and the Environment, Environmental Sciences Undergraduate Programme, University of Southampton, Highfield, Southampton SO17 1BJ, UK
[4] Present address: Haydale, Clos Fferws Parc Hendre, Ammanford SA18 3BL, UK
[5] Present address: University of Portsmouth, School of Biological Sciences, Portsmouth PO1 2DY, UK
[6] Present address: Center for Microbial Interface Biology, Departments of Microbial Infection and Immunity and Orthopaedics, The Ohio State University, Columbus, OH 43210, USA

E-mail: s.p.dennington@soton.ac.uk

Keywords: drag, biofilms, rheometer, roughness, sandpaper, rotating disc

OPEN ACCESS

RECEIVED
11 June 2015

REVISED
16 July 2015

ACCEPTED FOR PUBLICATION
7 August 2015

PUBLISHED
4 September 2015

Content from this work may be used under the terms of the Creative Commons Attribution 3.0 licence.

Any further distribution of this work must maintain attribution to the author(s) and the title of the work, journal citation and DOI.

Abstract

Frictional drag from the submerged hull surface of a ship is a major component of the resistance experienced when moving through water. Techniques for measuring frictional drag on test surfaces include towing tanks, flow tunnels and rotating discs. These large-scale methods present practical difficulties that hinder their widespread adoption and they are not conducive to rapid throughput. In this study a miniaturized benchtop rotating disc method is described that uses test discs 25 mm in diameter. A highly sensitive analytical rheometer is used to measure the torque acting on the discs rotating in water. Frictional resistance changes are estimated by comparing momentum coefficients. Model rough surfaces were prepared by attaching different grades of sandpaper to the disc surface. Discs with experimental antifouling coatings applied were exposed in the marine environment for the accumulation of microbial fouling, and the rotor was capable of detecting the increased drag due to biofilm formation. The drag due to biofilm was related to an equivalent sand roughness.

Introduction

Marine fouling

Marine fouling is the undesired accumulation of living organisms on ships' hulls and other manmade structures when these are immersed in the sea. Such fouling builds up inexorably on untreated ships' hulls and greatly increases frictional drag resulting in higher fuel consumption with an inevitable corresponding increase in carbon dioxide gas emissions. The economic consequences are severe, but difficult to quantify. The overall cost associated with hull fouling for the US Navy's mid-sized DDG-51 class destroyer fleet (22% of the navy's wetted hull area) was estimated by a unique study in 2010 to be $56M per year (Schultz *et al* 2011). A recent study (Eyring *et al* 2010) suggest that oceangoing ships consumed between 200 and 290 million metric tons of fuel in the year 2000, therefore at a present fuel cost of approximately $600 per tonne, each 1% increase in fuel consumption of the world's fleet equates to an expenditure of more than $1 billion. The attachment of marine organisms to ships' hulls also facilitates their translocation around the globe, and unwanted 'alien' species transported in this way can threaten biodiversity and cause real economic damage when they become established in new habitats. The costs of controlling the invasive zebra mussel in North America have been close to $1 billion over 10 years (De Poorter *et al* 2013).

Specialized antifouling paints are used on ship hulls below the waterline to combat the attachment of marine organisms. Traditional toxic antifouling paints containing biocidal ingredients (such as copper oxide and approved organic biocides) have proven very effective at preventing the attachment of fouling organisms. Non-toxic foul release coatings (FRC) are

© 2015 IOP Publishing Ltd

increasingly being used to avoid the problematic release of biocides into the marine environment. FRC have low energy ('non-stick') surfaces that macrofouling organisms such as barnacles and algae (seaweed) have difficulty in adhering strongly to, so that these loosely-attached organisms are removed by hydrodynamic forces when a ship reaches an operational speed of around 10 knots (Swain 1999). However, attached microbial fouling deposits known as biofilms, more commonly referred to as 'slime' by ship owners, form readily on FRC and are not removed even when a ship is under way at 30 knots (Candries *et al* 2001). The composition of marine biofilms has been reviewed (Salta *et al* 2013) and shown to consist largely of diatoms and bacteria, with pennate diatoms such as *Navicula* sp., *Nitzschia* sp. and *Licomophora* sp. dominating the biofilm. The increase in frictional drag due to even moderate biofilm coverage is considerable and has been estimated at 5% to 25% after 40 days and 240 days service respectively (Townsin 2003). Simple and rapid methods of measuring the drag due to biofilm are required.

Drag characterization methods for flat plates

Measuring the actual speed reduction of ships in service due to frictional drag is difficult, owing to the many challenges of collecting performance data and the lack of suitable controls. Therefore small-scale comparison methods using representative test surfaces must be used. Schulz (Schultz and Myers 2003) has compared three of the most common testing methods, namely towing tank tests, flow tunnels and rotating discs.

Towing tank tests operate by measuring the resistance to flow of a flat plate that is dragged through a large tank of water at speeds that simulate a moving vessel; the towing tank at the United States Naval Academy Hydrodynamics Laboratory described by Schultz (Schultz and Myers 2003) operates at up to 7.6 m s^{-1} (14.8 knots) velocity. To reach this speed and to enable sufficient data to be gathered the length of the tank is 115 m. Towing tank tests are complex to carry out and each run is time-consuming and expensive.

In flow tunnels the test surface is held static and water flows rapidly over it in a closed circuit system. The flow tank described by Schultz and Myers (2003) accepted test pieces 1.8 m in length with water flow velocity up to 6 m s^{-1} (11.7 knots). The velocity profile of the water flow over the surface was measured by laser Doppler velocimetry. The large size of the test plates is not conducive to testing expensive or difficult to apply coatings or other surface modifications.

Rotating disc drag characterization

Rotating disc methods are a simpler alternative to towing tanks and flow tests for characterizing the drag properties of test surfaces (Holm *et al* 2004). Discs are easily rotated in a tank of water, and high velocities, similar to those associated with ships, are attainable in a relatively compact apparatus. Rotation is by electric motor and the moment of force acting on the disc is measured by an in-line torque meter. Hydrodynamics are not well characterized since the flow varies across the surface. Cylindrical tanks are most commonly used but vortex flow is rapidly established in open cylinders without baffles. Tanks may need to be fully filled and enclosed to prevent the loss of water during high speed rotation and this complicates data analysis. Measurements are dependent on the geometry of the specific test rig.

Rotational rheometer drag characterization

Typical rotating disc rigs described in the literature used discs with diameters 23 cm (Schultz and Myers 2003) to 30 cm (Nelka 1973). These discs are rotated by an electric motor in cylindrical reservoirs containing volumes of water estimated at 20 L and 1000 L respectively. Tight fitting lids are required to prevent water being ejected from smaller reservoirs by rapidly rotating discs. Many of the handling issues associated with large rotating discs can be eliminated by a reduction in scale of the apparatus. However the drag forces generated on miniature discs are very low, which introduces unique measurement difficulties. We proposed the use of a sensitive rotational rheometer to measure the drag forces acting on discs of 25 mm diameter. Analytical rheometers are sensitive down to the μN m range of torque and have been previously used for measuring the frictional force on standard discs rotating in aqueous drag-reducing polymer solutions (Kim *et al* 2001). Small circular test coupons with varying surface conditions can be attached to the viscometer spindle and rotated in water at high angular velocities to measure the torque due to friction. Test coupons can be fabricated from a variety of materials, and experimental coatings may be applied to them by all standard methods including spin coating. We propose that multiple coated discs can be exposed simultaneously to marine fouling conditions by field exposure, giving the possibility of rapid throughput testing. For calibration purposes discs could have sandpaper of various grit sizes attached to their surface in order to establish the relationship between angular velocity and torque for different surface roughness in a similar manner to that of the Moody diagram which relates pressure drop (expressed as the non-dimensional friction factor) to flow velocity (expressed as the non-dimensional Reynolds numbers) for flow through rough pipes (Shockling *et al* 2006). In this way the degree of marine fouling could be expressed in terms of an effective roughness length scale.

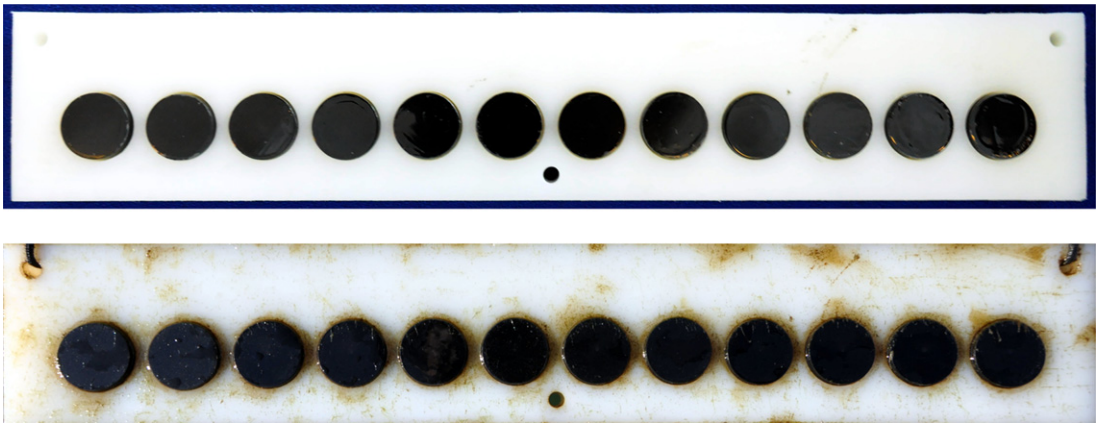

Figure 1. PTFE holder (377 mm × 70 mm) with 25 mm diameter sample coupons mounted. Before immersion (above), fouled after immersion (below). The brown appearance of the edges of the coupons before immersion is an optical artefact.

Materials and methods

Coupons: characterization and set-up

Test coupons were developed for antifouling sea exposure trials, fabricated from a 7.5 mm thick slice of 25 mm diameter rod made of black Delrin® (Du Pont) polyoxymethylene (POM or acetal) engineering thermoplastic. The high tensile strength and rigidity of POM combined with its low water absorption give the test coupons good dimensional and hydrolytic stability. An M3 screw thread was tapped into the centre of the rear side of each plastic coupon enabling attachment to a threaded rheometer spindle and fixing by an M3 nylon bolt in each well of the multiwell holder for ocean exposure.

Self-adhesive waterproof sandpaper discs of different roughness grades were fixed to the face of test coupons for calibration purposes. Circular discs with the same diameter as the test coupons were cut from commercial sandpaper sheets having a pressure-sensitive adhesive backing. To ensure that precise dimensions and a smooth edge were obtained, these discs were precision cut by a laser cutter (Laserscript LS6840, HPC Laser). The grades of red aluminium oxide sandpaper used were P240 (Faithfull Tools) and P120, P100, P80, P60 (Draper). Surface roughness of the discs was assessed by non-contact laser profilometry using an Alicona Infinite Focus Standard focus variation optical profiling microscope (Alicona Imaging GmbH). The roughness parameter used is Sa, the arithmetic average of the 3D roughness profile measured over a 20 mm zig-zag track made up of 10 continuous profile lines.

Experimental polymer coatings were applied to the face side only of discs by evaporation of polymer solutions. Poly(methyl methacrylate) (PMMA, mol. wt. 120 000, Sigma-Aldrich) was dissolved in toluene (low sulphur, Fisher Scientific) by stirring at 50 °C under nitrogen for 30 min to give a solution containing 30 wt% PMMA with viscosity 1770 mPa s at 25 °C (Brookfield CAP-2000+ cone and plate viscometer, cone no. 6 at 225 rpm). Approximately 2.2 g of polymer solution was spread onto a disc and the solvent was allowed to evaporate under ambient conditions, leaving a film of polymer approximately 120 μm thick. The amount of polymer applied was determined gravimetrically and the film thickness calculated knowing the density of the polymer.

Two compounds with potential activity against marine microbial fouling were investigated. These were cis-2-decanoic acid (Carbosynth),which is a short chain fatty acid (FA), and a proteolytic enzyme derived from pineapples, bromelain (BR) (Sigma-Aldrich). These compounds were dissolved and dispersed, respectively, in the PMMA solution and the two coatings were applied to discs, using the same procedure as the pure PMMA, to give films containing 2.4 wt% of each additive.

Hydrophobicity of coupons

The water contact angle on coatings applied to the test coupons was measured using a Kruss DSA100 goniometer and drop shape analysis software. Droplets of deionized water 1 μL in volume were placed on the surface of each test piece, centred 3 mm from the edge, using a motor-driven Hamilton syringe at 100 μL min^{-1}. The droplets (6 duplicates for each surface) were photographed 10 s after placement, at ambient temperature and humidity, and the software algorithm 'tangent 1' was used to determine the contact angle.

Test coupon sea immersion

Coupons to be exposed to fouling conditions in the sea were held in 25 mm diameter recesses in a flat poly (tetrafluoroethylene) (PTFE) plate by M3 nylon bolts screwed into the tapped hole for the rheometer mounting, with the surface of each disc held flush with the surface of the PTFE plate (figure 1). The plate with 12 coupons attached was immersed horizontally in the

sea at a depth of 1.5 m from the seawater surface from 24th August 2012 to 3rd September 2012 (9 days) at the National Oceanography Centre Southampton (NOCS), latitude 50°53′28N longitude 1°23′38W. After sea exposure a small amount of biofilm had formed on the surface of the coupons, more easily visible on the white PTFE holder which showed a patchy distribution of green/brown biofilm (figure 1). The patchy appearance of biofilms on the holder could indicate grazing by fish, and measures to prevent this will be taken in future. There is no fouling growth on the sides of the coupons as these are protected within the holder, allowing the surface roughness alone to be compared to equivalent sandpaper roughness grades. The coupons were recovered and those intended for rheometer drag testing were stored immersed in artificial seawater (ASW), in a container placed on wet ice to prevent further growth or deterioration.

Rheometer set up and description

A rheometer type AR-G2 (TA Instruments) with a magnetic thrust-bearing was adapted for measuring the ultra-low torque on sample discs rotating in water. According to the instrument manufacturer, the torque measurement range of this rheometer for 'steady shear' measurements is 0.01 μN m to 200 mN m with a resolution of 1 nN m. An M3 screw-threaded stainless steel connector rod, passing through the rheometer, was screwed into the threaded hole in the rear face of a disc, thereby clamping it to the rotating part of the instrument. The rheometer body was then lowered to immerse the disc in water. Any air bubbles trapped below the horizontal test face of the disc were removed by suction using a glass Pasteur pipette with the tip bent upwards in a U-shape. A cylindrical reservoir (Fisher, tall form 600 mL glass beaker) filled with water to a depth of 7 cm was evaluated but rejected for use as a reservoir as significant vortex flow was established even at moderate angular velocity, leading to water being ejected from the container. Discs could however be rotated in a cubic clear acrylic reservoir with 9.4 cm sides (internal measurement) and water depth 7 cm at up to 300 rad s^{-1} (2865 rpm) without causing splashing or significant vortexing, and this system was adopted for all tests. This was approximately the largest square reservoir that could be fitted into the space available, limited by the structure of the instrument. The gap between the lower surface of the disc and the floor of the cube was fixed at 1 cm after initial trials to determine the effect of gap size on flow patterns and torque sensitivity. Flow patterns were visualized by adding neutral buoyancy polymer beads of two contrasting colours, blue and orange (Cospheric LLC, Santa Barbara, CA, USA) and photographed using a digital camera (Olympus C-5050) at a shutter speed of 1/30 s. For recording torque data the disc angular velocity was increased linearly from standstill to 300 rad s^{-1} over 60 s and rotation was maintained for 30 s at the highest speed before decreasing to zero angular velocity linearly over 60 s.

Calculation

The moment or torque coefficient (C_m) of a rotating disc is a dimensionless number defined by (Granville 1982):

$$C_m = \frac{2M}{\rho \cdot r^5 \cdot \omega^2}, \quad (1)$$

where M is the torque acting on the whole disc, ρ is the density of the fluid, r is the radius of the disc and ω is the angular velocity.

$$\text{Rearranging, } M = k \cdot C_m \cdot \omega^2, \quad (2)$$

where:

k is a constant for the system $\left(\frac{\rho \cdot r^5}{2}\right)$.

For a disc rotating in a constrained volume of fluid, a mean tangential swirling or vortex flow may be induced, which reduces the effective angular velocity of the disc. To compensate for this a 'swirl factor' (φ) may be determined (Granville 1982) with value $0 < \varphi < 1$ relating the conditions to those obtaining in an unenclosed volume of fluid. The effective angular velocity then becomes $\varphi\omega$. This calibration was not performed by us ($\varphi = 1$), due to the structure of the instrument making measurements with larger reservoirs not possible, and only the relative changes in torque due to drag were considered.

Torque (M) over the angular velocity (ω) range between 200 and 300 rad s^{-1} was plotted against ω^2 for each disc condition. In this turbulent flow regime the drag shows a close to quadratic angular velocity dependence and the data could be fitted to a straight line having slope ($k \cdot C_m$). Values of C_m in this velocity range were compared to indicate the effect of different surface roughness conditions.

Results

Torque measurements

The flow pattern in the cubic water reservoir with a 25 mm diameter blank Delrin disc rotating at 275 rad s^{-1}, made visible by the motion of blue and orange neutral density beads during a 1/30 s exposure, is shown in figure 2. There was minimal vortexing around the shaft, and turbulent flow with good mixing throughout the volume of water.

This rheometer configuration was used to measure the torque generated on blank 25 mm diameter Delrin discs rotating in ASW. The angular velocity was increased from standstill to 300 rad s^{-1} over 60 s while the torque was continuously recorded. The slope of the torque against angular velocity increases regularly with no chaotic change that would indicate a transition from laminar to turbulent flow regimes, while at angular velocity $\geqslant$200 rad s^{-1} the torque can be taken

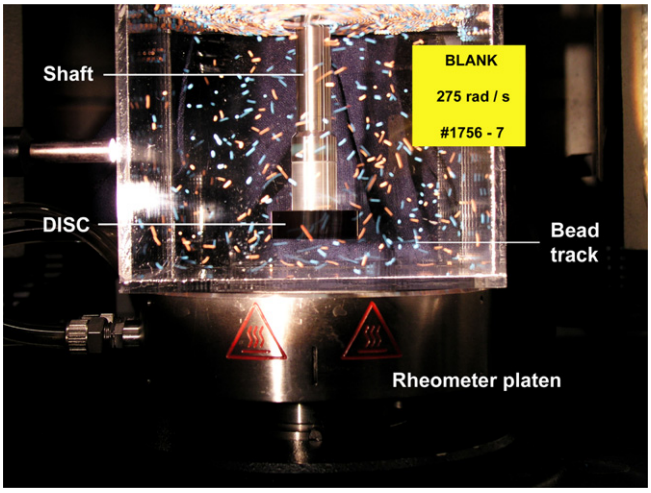

Figure 2. Flow patterns with neutral density beads, blank 25 mm diameter disc at 275 rad s^{-1}, exposure 1/30 s.

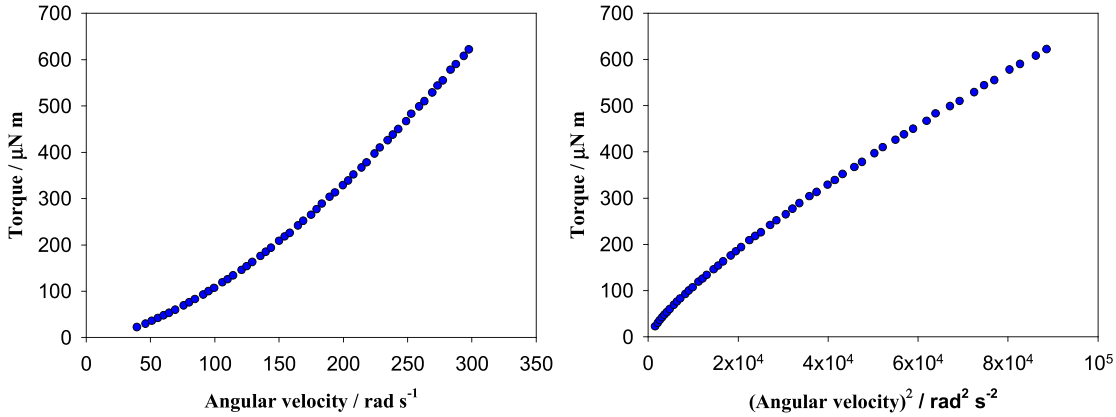

Figure 3. Torque data for blank 25 mm diameter Delrin discs (average of 5 runs). (Left) raw data showing torque as a function of ω. (Right) data was linearized by plotting torque against $(\omega)^2$ demonstrating a 2nd order power law relationship above $\omega = 200$ rad s^{-1} (4×10^4 rad^2 s^{-2}).

as varying linearly with the square of the rotational velocity (figure 3). Therefore torque data in the rotational range of 200–300 rad s^{-1} (1910–2865 rpm) were used for calculation of the momentum coefficient. The rotational Reynolds Number varies from 3.0×10^4 to 4.5×10^4 over this velocity range.

Sandpaper calibration

The rheometer set-up was calibrated using each size of disc by measuring the torque on coupons with discs of self-adhesive sandpaper attached. The mean torque (M) acting on replicate discs for each sandpaper grade was plotted against ω^2 (figure 4) over the angular velocity range $\omega \geqslant 200$ rad s^{-1}. Linear regression gave the slope ($= k \cdot C_m$) which yields the dimensionless, C_m when divided by the appropriate value of k (table 1). For 25 mm diameter discs in ASW with density 1025 kg m^{-3}, $k = 1.564 \times 10^{-7}$ kg m^2.

The torque data for the P80 and P100 grade sandpaper surfaces were very close to each other, and the measured Sa values confirmed that the two grades had a similar surface roughness of 38.4 μm and 38.7 μm respectively. In figure 5 the coefficient of momentum is plotted against the measured surface roughness derived from two duplicate discs, with a linear trendline shown.

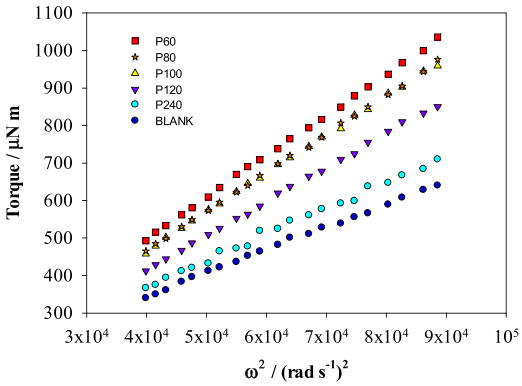

Figure 4. Torque versus ω^2 for 25 mm diameter Delrin discs with sandpaper-covered surface.

Table 1. Coefficient of momentum derived by linear regression.

25 mm	BLANK	P240	P120	P100	P80	P60
Sa/μm:	1.4	13.8	27.7	38.7	38.4	45.5
Slope:	6.09E-09	6.96E-09	9.10E-09	1.03E-08	1.03E-08	1.09E-08
C_m:	3.90E-02	4.45E-02	5.82E-02	6.58E-02	6.60E-02	7.00E-02
SD (n)	1.81E-03 (3)	7.93E-04 (2)	2.78E-03 (3)	1.72E-03 (2)	9.81E-04 (2)	1.05E-03 (2)
SD % mean	4.64	1.78	4.78	2.61	1.49	1.5
p-value	—	0.029	0.001	0.000	0.000	0.000

Note: SD (n) = sample standard deviation (number of samples) and p-value from two-tailed t-test comparing C_m with sandpaper to that of blank disc.

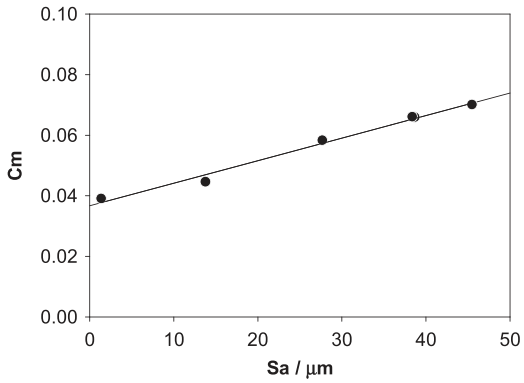

Figure 5. Coefficient of momentum versus measured surface roughness.

Table 2. Water contact angle and standard deviation of the polymer-coated disc surfaces.

Water contact angle		
Coating type	Degrees	SD (10)
PMMA	80.7	1.03
PMMA + FA	83.0	1.31
PMMA + BR	79.9	1.56

The value of C_m calculated from the torque data can be fit to the surface area roughness (Sa) of the sandpapers by the linear relation:

$$C_m = 7.458\text{E} - 04\ \text{Sa} + 3.668\text{E} - 02\left(R^2 = 0.988\right). \quad (3)$$

It is noted that the disc geometry is complex, and C_m is influenced not only by the test surface but also the 7.5 mm depth perimeter of the disc, the disc's upper surface and also the immersed length of the rotating rod to which the disc is attached. These additional surfaces presumably complicate the analysis beyond that of the analysis by Granville.

Experimental antifouling-coated coupons

Coupon characterization

The water contact angle of the clean polymer-coated disc surfaces is given in table 2.

The presence of the 120 μm thick PMMA-based coatings on the discs gave a small increase of approximately 4% in C_m compared to the uncoated discs. This increase could possibly be due to the increased thickness or weight contributed by the coating rather than to any change in surface roughness. It was not possible to measure the actual surface roughness of the coated discs using optical profilometry owing to intense light reflection from the clear, glass-like surfaces. Visually the surfaces appeared smooth.

The Delrin discs recovered after 9 days of exposure in the sea had a light covering of microfouling (slime) visible to the naked eye, as did the PTFE holder. The covering on the holder was patchy, indicating possible predation by fish grazing on biofilm. Representative fouled coupons were air-dried and sputter coated with gold and the fouling organisms were examined using a scanning electron microscope (SEM) (JEOL JSM-5600LV) (figure 6).

The measured C_m values for the clean discs and the fouled discs is given in table 3 along with the equivalent sandpaper roughness (Sa) calculated from the 25 mm disc regression equation. The equivalent roughness values are plotted in figure 7 where the dotted line indicates the mean equivalent roughness (3.79 μm) of the clean discs.

Discussion

Objects moving through a resistive medium experience an opposing force which is related to their velocity in either a linear or quadratic fashion depending on the Reynolds number (Re) (Timmerman and van der Weele 1999). Thus, a small sphere falling through a viscous liquid under the force of gravity (at very low Re) experiences drag linearly proportional to its velocity as described by Stokes law.

$$F_d = 6\pi\ \mu\ R\ \upsilon, \quad (5)$$

where F_d is the drag force, μ is the dynamic viscosity of the liquid, R is the radius of the sphere and ν is the velocity of the sphere.

A sphere moving through a fluid at high velocity resulting in turbulent flow (i.e. at high Re) will experience drag varying as the square of the velocity according to Rayleigh's equation

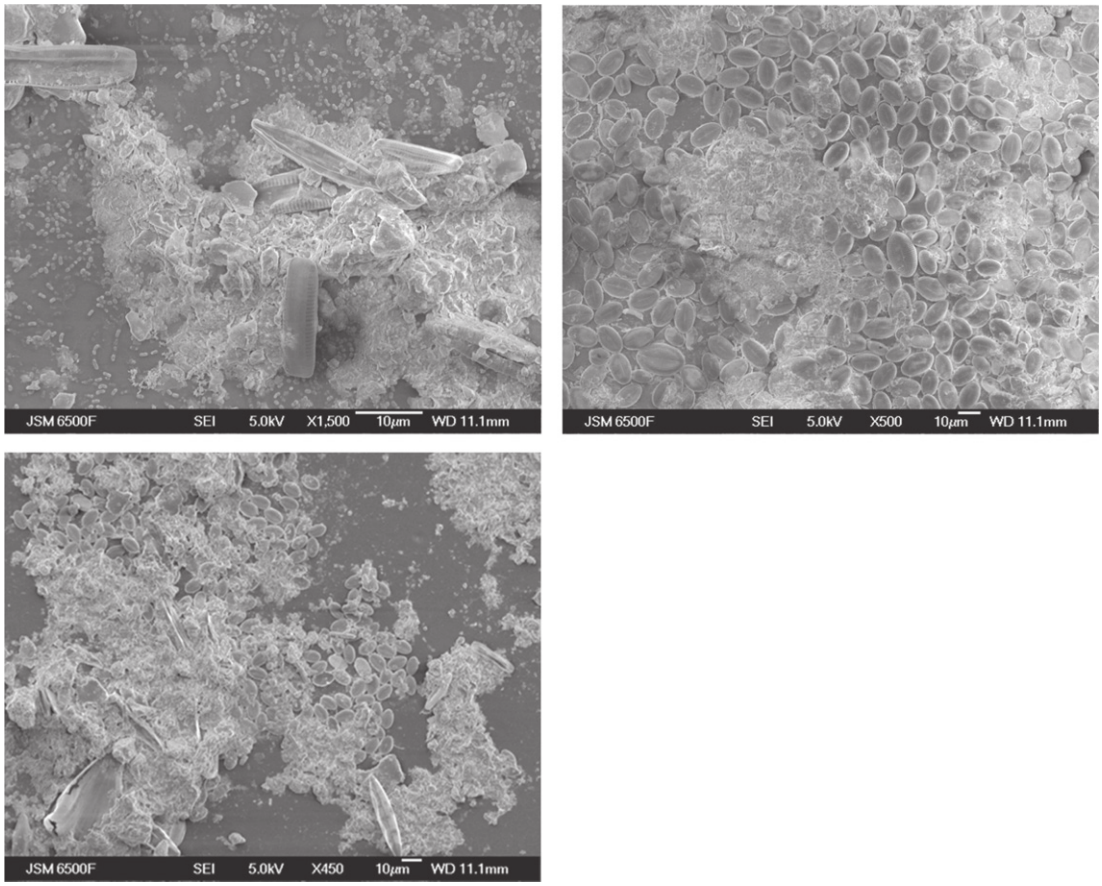

Figure 6. SEM micrographs of the PMMA surface (top left), PMMA + FA (top right) and PMMA + BR (bottom). The surfaces were colonized with pennate diatoms having various frustule morphologies, including *Amphora* sp. and *Navicula* sp. On the PMMA + FA short bacterial rods were also present but they were not seen in all locations on the surface. There was little difference in the thickness (considering dehydration) but the PMMA + BR appeared to have the densest covering composed mainly of diatoms.

Table 3. C_m and Sa for clean and biofilmed coupons.

Coating	CLEAN C_m	FOULED C_m	CLEAN Sa	FOULED Sa	Change in Sa %	*p*-value for Sa fouled versus Sa clean
PMMA1	3.96E-02	4.22E-02	3.92	7.49	91.24	
PMMA2	3.95E-02	4.28E-02	3.82	8.25	116.22	0.034
PMMA + FA1	3.96E-02	4.20E-02	3.99	7.21	80.57	
PMMA + FA2	3.96E-02	3.94E-02	3.92	3.74	−4.51	0.267
PMMA + BR1	3.95E-02	4.37E-02	3.79	9.35	146.96	
PMMA + BR2	3.91E-02	4.77E-02	3.33	14.73	342.11	0.105
Mean	3.95E-02	4.30E-02	3.79	8.46	128.76	
SD	1.80E-04	2.72E-03	0.24	3.60	116.19	

Note: FA = fatty acid, BR = bromolein, SD = sample standard deviation and *p*-value from paired one-tailed *t*-test comparing duplicate fouled coupons with duplicate clean coupons.

$$F_d = \frac{1}{2}\,\rho\,v^2\,C_d A, \tag{6}$$

where F_d is the drag force, ρ is the density of the fluid, ν is the speed of the object relative to the fluid, A is the cross-sectional area and C_d is the drag coefficient—a dimensionless number.

A similar relationship also holds for fluid flow in pipes, where the head loss (or pressure drop) is proportional to the square of the velocity in turbulent flow according to the Darcy formula (Massey 2012). We observed that the torque acting on our rotating discs varied as the square of the angular velocity at speeds >200 rad s^{-1}. This quadratic relationship between ω and M in this work is therefore analogous to that for both spheres and for turbulent pipe flow even though our highest *Re* is transitional. The motion of neutral density beads indicated turbulent flow patterns with a stable Taylor-like vortex pair having an axis of rotation parallel to the plate. Owing to the choice of a cubic rather than cylindrical container no splashing and only minimal vortexing of the water occurred, even at maximum rotational velocity. This simplifies the experimental procedure and may reduce the need for an empirical 'swirl factor' when calculating the momentum coefficient.

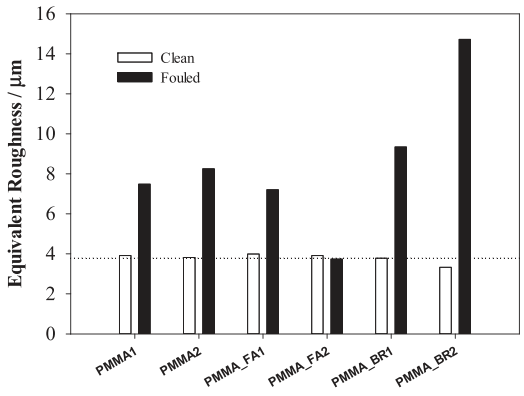

Figure 7. Equivalent sandpaper roughness of experimental antifouling coatings.

Holm *et al* (Holm *et al* 2004) used the percentage change in the frictional resistance coefficient (C_f) of a rotating disc to measure the drag penalty due to accumulated biofilms on experimental FRC. The similarity-law characterization method developed by Granville (1978, 1982) was used to derive the roughness functions (ΔB versus $k*$) from the measured momentum coefficients and the roughness functions were converted to frictional resistance coefficients through Granville's iterative process based on the similarity of the boundary layers of rough and smooth walls. A Reynolds number corresponding to a 100 m flat plate was chosen as being representative of the length of a ship for this conversion. Our attempts to use the similarity index did not result in a good relationship with surface roughness. It is unclear whether this is due to the geometry of the discs or to the fact that we were not fully in the turbulent regime. We have therefore chosen to use the percentage change in (C_m) to compare frictional drag penalties. C_m is a simple parameter to calculate and was found to be constant over the range of angular velocities studied (200–300 rad s^{-1}). However the absolute value of C_m is dependent on the geometry of the measurement system of disc and shaft.

The drag due to different grades of sandpaper attached to disc surfaces could be correlated with their measured surface roughness as determined by optical profilometry. The most relevant measure of surface roughness was Sa, which showed a linear relation with C_m. The value of Sa extrapolated from the linear sandpaper calibration curves for the blank 25 mm discs was close to the roughness measured by optical profilometry (3.8 μm compared to 1.4 μm).

The derived relation of C_m to measured surface roughness for a fixed disc rotor geometry enables unknown surface textures (e.g. from marine fouling) to be related to equivalent standard sandpaper roughness values. The use of a FA and an enzyme (BR) as experimental antifouling agents was a first attempt at assessing the rheometer methodology for detecting antifouling active coatings. After sea exposure all fouled discs except for one duplicate of the FA-containing PMMA coating showed greater sandpaper equivalent roughness compared to the clean state of the discs, and the mean increase over all discs was significant ($p = 0.015$, paired one-tailed t-test). The apparent degree of microfouling on discs with the same coating varied greatly between the two duplicates exposed. This is to be expected in any biological growth experiment. Duplicate exposures are clearly inadequate to assess the degree of biofilm fouling accumulated, and the results presented here are purely to demonstrate that the method is capable of detecting and quantifying small changes in surface roughness due to biofilm.

Interestingly, both BR-containing coatings showed the heaviest microfouling coverage. One speculative explanation is that the protease activity might have digested naturally occurring proteins in the water providing amino acids at the surface possibly stimulating growth. For future studies, in addition to increasing the sample number, it is also important to confirm bioactivity of the active agent when incorporated into a coating as well as characterizing the release kinetics.

The increase in drag due to even the thickest biofilm observed in this exposure series was only comparable to the finest grade 240 sandpaper, with an equivalent sandpaper roughness of approximately 12 μm. The thickness of the biofilm appeared much greater than this by visual inspection, but the discrepancy could be due to the patchiness of the biofilm coverage. The low equivalent roughness could also be connected with the viscoelasticity of the biofilm and this interesting possibility will be explored in further work.

The small scale of the test will limit its use largely to fouling by microbial slime and it will not be suitable for assessing the drag due to larger organisms or colonies of organisms such as sea squirts, barnacles, etc whose size scale and pattern distribution is larger than the discs themselves. In this respect the small discs may only be appropriate for assessing the potential efficacy of coatings to reduce or prevent microbial slime in the early stages of exposure. The analytical rheometer is sufficiently sensitive to measure the minute changes in drag due to a thin accumulation of microbial fouling, and we are currently working on using optical coherence tomography and other methods to quantify the fouling layer so that we can make better interpretation between the change in drag and the amount of biomass.

Conclusion

The method described here is simple and rapid to carry out. The small size of the discs and the low volume of water required to rotate them in (<1 L) eliminates the handling problems associated with large disc rotors while producing data of comparable utility. The lack of

vortexing and swirling of the water in a cubic container increases confidence in the data obtained and may eliminate the need for considering an empirical swirl factor.

Calibration using discs bearing known sandpaper textures was straightforward, and allows comparison of fouled disc surfaces with those of known surface roughness. Calibration results apply to a specific measurement geometry and disc diameter only. An important consideration is the sensitivity of the analysis to variables in the experimental set-up. Temperature and density of the water in the tank are easily controlled in the laboratory and have only minor effects on torque. A potential source of variation is the fact that the torque is proportional to the radius of the disc raised to the fifth power. This means that the value of C_m is extremely sensitive to small changes in effective disc radius, e.g. such as would be caused by fouling adhering to the edge of the disc.

The rheometer used was found to be capable of registering the increased drag due to a thin covering of microfouling developed over only 9 days sea immersion on a small sample disc. It could also differentiate between the amounts of microfouling accumulated on different experimental antifouling coatings. A coating containing dispersed BR enzyme appeared to foul more than a blank coating or one containing a short chain FA, however duplicate disc exposures of the potential antifouling coatings gave highly varying results for the amount of biofilm accumulated. This is to be expected for any biological process, and multiple discs should be exposed.

Future work will compare these data with those obtained from a conventional large disc rotor rig and ultimately with those from a flat plate in a towing tank. The aim will be to mathematically relate the hydrodynamic drag measured in the different test systems to each other using a scaling factor analysis.

Acknowledgments

The authors gratefully acknowledge financial support from the EPSRC grant EP/J001023/1 (Green Tribology), the National Physical Laboratory, the Knowledge Transfer Partnership between the University of Southampton and Haydale Limited (Technology Strategy Board Project 508710), and the University of Southampton Engineering Sciences MSc programme. Data supporting this study are openly available from the University of Southampton repository at http://dx.doi.org/10.5258/SOTON/379269.

References

Candries M, Atlar M and Anderson C D 2001 Foul release systems and drag *Consolidation of Technical Advances in the Protective and Marine Coatings Industry*, *Proc. PCE 2001 Conf.* (*Antwerp*) pp 273–86

De Poorter M, Darby C and MacKay J 2013 Marine menace—alien invasive species in the marine environment *International Union for Conservation of Nature*

Eyring V, Isaksen I S A, Berntsen T, Collins W J, Corbett J J, Endresen O, Grainger R G, Moldanova J, Schlager H and Stevenson D S 2010 Transport impacts on atmosphere and climate: shipping *Atmos. Environ.* **44** 4735–71

Granville P S 1978 Similarity-law characterization methods for arbitrary hydrodynamic roughnessses *David W Taylor Naval Ship Research and Development Center* (Bethesda, Md) Report no. 78-SPD-815-01

Granville P S 1982 Drag characterization method for arbitrarily rough surfaces by means of rotating disks *J. Fluids Eng.* **104** 373–7

Holm E, Schultz M, Haslbeck E, Talbott W and Field A 2004 Evaluation of hydrodynamic drag on experimental fouling-release surfaces, using rotating disks *Biofouling: J. Bioadhesion Biofilm Res.* **20** 219–26

Kim C A, Jo D S, Choi H J, Kim C B and Jhon M S 2001 A high-precision rotating disk apparatus for drag reduction characterization *Polym. Test.* **20** 43–8

Massey B S 2012 *Mechanics of Fluids* 9th edn (Boca Raton, FL: CRC) p 248

Nelka J N 1973 *Evaluation of a Rotating Disk Apparatus: Drag of a Disk Rotating in a Viscous Fluid* (US Naval Academy) p 50

Salta M, Wharton J A, Blache Y, Stokes K R and Briand J-F 2013 Marine biofilms on artificial surfaces: structure and dynamics *Environ. Microbiol.* **15** 2879–93

Schultz M P and Myers A 2003 Comparison of three roughness function determination methods *Exp. Fluids* **35** 372–9

Schultz M P, Bendick J A, Holm E R and Hertel W M 2011 Economic impact of biofouling on a naval surface ship *Biofouling* **27** 87–98

Shockling M A, Allen J J and Smits A J 2006 Roughness effects in turbulent pipe flow *J. Fluid Mech.* **564** 267–85

Swain G 1999 Redefining antifouling coatings *J. Protective Coat. Linings* **16** 26–35

Timmerman P and van der Weele J P 1999 On the rise and fall of a ball with linear or quadratic drag *Am. J. Phys.* **67** 538–46

Townsin R L 2003 The ship hull fouling penalty *Biofouling* **19** (suppl.) 9–15